Zeolite Synthesis

A Titanosilicate That Is Structurally Analogous to an MWW-Type Lamellar Precursor**

*Weibin Fan, Peng Wu, Seitaro Namba, and Takashi Tatsumi**

Titanosilicate catalysts are of scientific and technological interest because of their ability to be applied to environmentally friendly chemical processes for the liquid-phase catalytic oxidation of a variety of organic compounds, by using H_2O_2 as a clean oxidant. The medium-sized pore

---

[*] Dr. W. Fan, Dr. P. Wu, Prof. T. Tatsumi
Division of Materials Science & Chemical Engineering
Graduate School of Engineering, Yokohama National University
Tokiwadai 79-5, Yokohama 240-8501 (Japan)
Fax: (+81) 45-339-3943
E-mail: ttatsumi@ynu.ac.jp

Prof. S. Namba
Department of Materials, Teikyo University of Science and Technology, Uenohara-machi, Yamanashi 409-0193 (Japan)

[**] This work was supported by Core Research for Evolutional Science and Technology of Japan Science and Technology Corporation. W.F. gratefully acknowledges Japan Society for Promotion of Science (JSPS) for a fellowship as a foreign researcher.

Supporting information for this article is available on the WWW under http://www.angewandte.org or from the author.

DOI: 10.1002/ange.200352723

openings of TS-1 render it inactive for the oxidation of lager molecules.[1] Therefore, many efforts have been made to develop large-pore titanosilicates to meet increasing demands for synthesizing fine chemicals in an environmentally friendly way. For this purpose, Ti-Beta, Ti-MTW, Ti-MOR, and Ti-ITQ-7, all with 12-membered-ring (12-MR) pores, as well as Ti-containing mesoporous materials have been prepared.[1–5] However, none of these catalysts are efficient enough in terms of intrinsic activity and stability. Recently, Ti-MWW has proved to be much more active than TS-1 and Ti-Beta in the epoxidation of linear alkenes with H_2O_2,[6] but unfortunately for the oxidation of bulky molecules, it is still inferior to Ti-Beta owing to severe steric restrictions. Actually, with respect to MWW-type materials, potential advantages are expected from their supercages and side pockets, but access to the supercages is seriously restricted by the openings of the elliptical 10-MR pores once the three-dimensional (3D) MWW crystalline structure is formed from the lamellar precursor. Thus, Corma et al. delaminated an MWW zeolite into isolated crystalline sheets by a rather complicated method, and then grafted on titanocene to obtain Ti/ITQ-2.[7] However, this material can only achieve high reactivity and epoxide selectivity with organic hydroperoxide oxidants under extremely harsh conditions (that is, the absence of water in the system), probably as a result of the presence of a large number of hydrophilic silanol groups that reside on the exterior surface. From the geometrical point of view, the retention of a lamellar structure with a layer spacing not less than that of an as-synthesized MWW precursor after calcination would be an alternative way for creating the open space required for reactions. Thus prepared materials not only make the active sites within the supercages more accessible to bulky molecules but are also endowed with the capability of promoting the oxidation reactions with an aqueous solution of H_2O_2 as an oxidant. This would open new possibilities for titanosilicates to be applied to fine-chemical industry. We have succeeded in preparing such a novel titanosilcate catalyst (denoted as Ti-YNU-1), and have found that this material shows substantially improved oxidation ability, epoxide selectivity, and stability in the liquid-phase epoxidation of cycloalkenes.

Figure 1 shows the XRD patterns of as-synthesized samples of 3D Ti-MWW and Ti-YNU-1. The as-synthesized sample had the structure of an MWW lamellar precursor, as evidenced by the presence of peaks due to the 001 and 002 reflections (Figure 1 a). A 3D MWW framework was formed upon direct calcination as a result of condensation of hydroxyl groups between the layers (Figure 1 b). In contrast, the layer structure was still retained when the as-synthesized material was refluxed in acid solution and further calcined (Figure 1 c and d). When compared with 3D Ti-MWW, the diffraction lines associated with the c crystallographic axis are all shifted to lower values of 2θ for Ti-YNU-1. This indicates that the unit-cell parameter c had increased.[8] Indeed, the c parameter of Ti-YNU-1 was 27.47 Å, in contrast to 24.98 Å for the corresponding 3D structure, while both samples showed similar a and b parameters. Since the crystalline structure within the layers is highly rigid, it is reasonable to suggest that the increase in the c parameter is mainly due to the expansion of the layer spacing by about 2.5 Å.

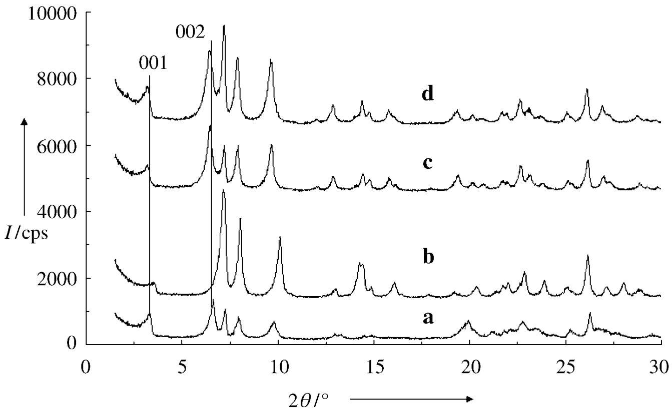

Figure 1. XRD patterns of a) the as-synthesized lamellar precursor of Ti-MWW, b) the directly calcined material (3D Ti-MWW), c) an acid-treated sample and d) the same sample after calcination (Ti-YNU-1).

Figure 2 shows high-resolution transmission electron micrograph (HRTEM) images of the edge-on view of the crystallites. The thickness of every 10 layers in Ti-YNU-1 is comparable to that of 11 layers in 3D Ti-MWW. Considering that the single-layer thickness for 3D MWW zeolites is about 25 Å, the TEM images visually demonstrate that Ti-YNU-1 has an interlayer spacing enlarged by about 2.5 Å, in agreement with the XRD characterization. This structure is totally

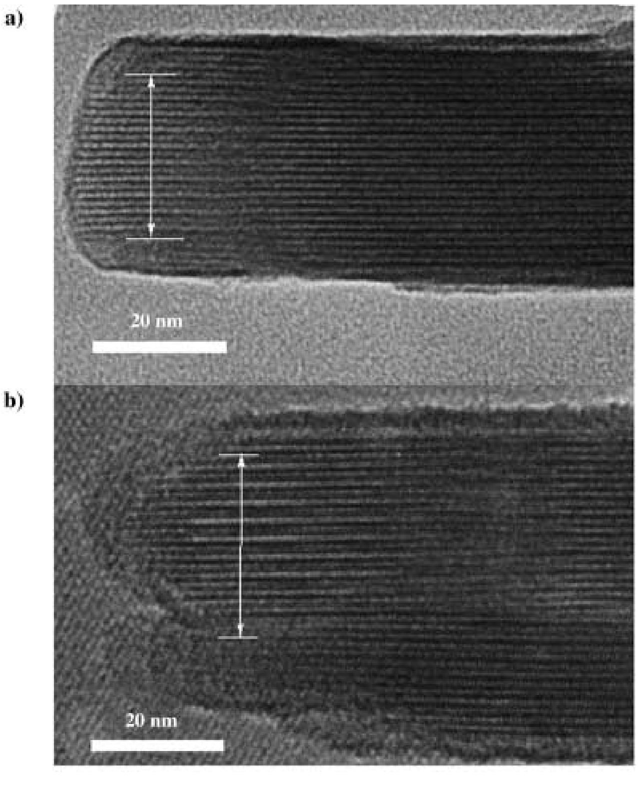

Figure 2. Edge-on TEM images of 3D Ti-MWW (a) and Ti-YNU-1 (b). (The arrow indicates the thickness of 10 layers.)

different from ITQ-2, which is composed of separate layers.[9] In contrast, Ti-YNU-1 possesses a lamellar structure that is analogous to the MWW-type precursor although the linkage between the layers after removing the templating molecules is not fully determined at the moment. The possibility that the layers are pillared by a small amount of Ti that remains after acid treatment can be excluded because the lamellar structure (Si-YNU-1) was still formed under similar synthesis conditions even when titanium was not added to the synthesis gel. The diffraction lines of ITQ-2 are very weak in intensity and almost indiscernible,[9] whereas those of Ti-YNU-1 are similar to those of 3D Ti-MWW. This result shows that their structures are completely different. The former lacks long-range periodicity, while the latter completely retains this property. In addition, the delamination process also inevitably led to the partial destruction of the crystalline-sheet structure, and consequently affected the catalytic performance.

The formation of a lamellar structure depends heavily on the amount of Ti present in the synthesis gel. When the Si/Ti ratio in the synthesis gel was greater than 50, the lamellar structure appeared gradually with decreasing Ti content after acid treatment and subsequent calcination. In contrast, the 3D MWW structure was only formed at lower Si/Ti ratios (e.g., ≈ 30). The surface area and pore volume of Ti-YNU-1 are about 676 $m^2 g^{-1}$ and 0.202 $mL g^{-1}$, whereas those of 3D Ti-MWW are only 528 $m^2 g^{-1}$ and 0.154 $mL g^{-1}$, respectively. This supports the substantial expansion of the layer space. The N_2 adsorption/desorption isotherms show that Ti-YNU-1, like 3D Ti-MWW, displays typical behavior of microporous materials with an external surface area of about 61.4 $m^2 g^{-1}$, which confirms that it is a well-crystalline molecular sieve. In contrast, ITQ-2 shows a significantly high mesopore volume and an external surface area of about 700 $m^2 g^{-1}$.[9] This provides more evidence that Ti-YNU-1 possesses a structure different from that of ITQ-2 or Ti/ITQ-2.

Compared with the 3D Ti-MWW sample, Ti-YNU-1 showed a more intense band in the OH-vibration region of the FTIR spectrum (3728 cm^{-1}), which is probably ascribed to asymmetric hydrogen-bonded silanols.[10] Furthermore, the ^{29}Si MAS NMR spectrum of Ti-YNU-1 showed a signal at 88.6 ppm, which is characteristic of Q^2 ($Si(OH)_2(OSi)_2$) and/or $Si(OH)(OTi)(OSi)_2$ and was absent for 3D Ti-MWW. The presence of a large number of silanol groups in Ti-YNU-1 was also proved by H_2O adsorption at 298 K. The amount of the adsorbed water on Ti-YNU-1 was about four times as large as that on 3D Ti-MWW. Nevertheless, diffuse reflectance UV/Vis spectroscopy shows that all of the Ti atoms in Ti-YNU-1 are tetrahedrally coordinated, as evidenced by the presence of a band at ≈ 210 nm but no bands above 250 nm that could be attributed to octahedrally coordinated Ti and titanium oxides.[11] For Ti/ITQ-2, the grafted Ti is merely located at the external surface, but not in truly isomorphous substituted lattice sites; hence, it is similar to Ti-MCM-41, which is also prepared via the grafting method.[12] This probably accounts for the fact that epoxidation of cyclohexene can only be carried out without water present, while Ti/ITQ-2 serves as a catalyst.[7]

The reason for the formation of Ti-YNU-1 is not clear. The presence of silanol groups, related to defect sites not occupied by Ti at high Si/Ti ratios, is tentatively presumed to cause the stacking faults when the intercalated piperidine was removed by acid treatment, which then gives rise to a layered structure even after further calcination. With an increase in Ti content in the gel, more Ti atoms would be incorporated into the T_1 positions of the proposed structure.[13,14] The stacking faults would be thus eliminated since the Ti–OH bond (1.95 Å) is much longer than Si–OH bond (1.61 Å), and incorporation of Ti in T_1 sites constricts the T-O-T angle so that it is more acute than the Si-O-Si angle in pure silicates.[15] The scheme for the formation of Ti-YNU-1 is illustrated in Figure 3.

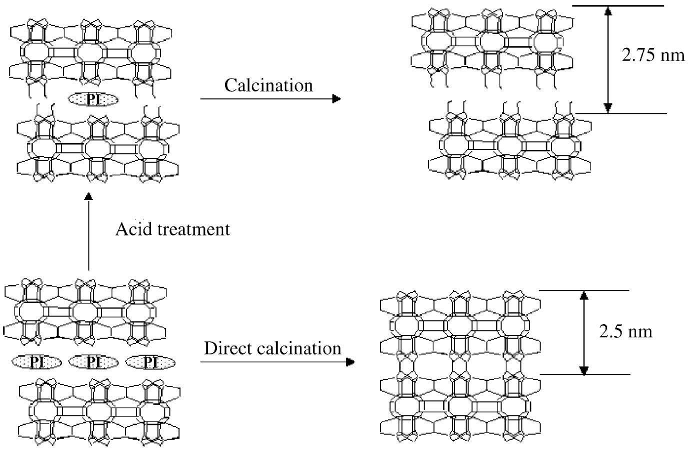

Figure 3. Possible scheme for the formation of Ti-YNU-1 and 3D Ti-MWW, as well as their structures. Direct calcination of the as-synthesized lamellar precursor burns off the organic species and subsequently leads to dehydroxylation between the layers and hence formation of 3D MWW structure. However, the acid treatment washes out most of the organic species, which causes stacking faults due to the presence of silanols on defect sites. Ti-YNU-1 with a lamellar structure is then obtained even after subsequent calcination.

Table 1 summarizes the catalytic results for the oxidation of cyclohexene over various titanosilicates. Compared with Ti-Beta, Ti-YNU-1 not only exhibited a higher activity but also gave much higher epoxide selectivity. 3D Ti-MWW showed a moderate conversion, whereas TS-1 and Ti-MOR were less active. This indicates that among the typical titanosilicates, Ti-YNU-1 is the most active and selective catalyst for the oxidation of cyclohexene irrespective of the lowest Ti content. The stability of the catalyst was investigated by repeating the reaction eight times. The used Ti-YNU-1 catalyst gave a cyclohexene conversion and an epoxide selectivity in the range of 31.5–34.5 % and 87.5–92.8 %, respectively, after being regenerated by calcination in air at 773 K. In contrast, the conversion on Ti-Beta decreased by 23 % when subjected to only three repeated reaction runs.

The turnover number (TON) for the oxidation of different clycloalkenes catalyzed by various titanosilicate molecular sieves is depicted in Figure 4. TS-1 exhibited high activity for the oxidation of cylopentene, while the activity declined drastically in the case of cyclohexene, and even more severely with increasing molecular size of cycloalkenes, due to increasing steric restrictions. Although 3D Ti-MWW showed

Table 1: Catalytic activity of various titanosilicates in the oxidation of cyclohexene.[a]

Catalyst	Si/Ti	Conv. [%]	Selectivity [%]		H_2O_2
			Epoxide	Others[b]	Selectivity [%]
TS-1	83	3.3	17.9	82.1	n.d.
3D Ti-MWW	45	8.1	35.0	65.0	74.8
Ti-MOR[c]	92	9.0	55.0	45.0	63.5
Ti-Beta	35	16.5	78.4	21.6	51.6
Ti-YNU-1	240	21.2	90.8	9.2	78.5

[a] Reaction conditions: catalyst (0.05 g), acetonitrile (10 mL), cyclohexene (10 mmol), H_2O_2 (10 mmol; 31 % aqueous solution), 333 K, 2 h. [b] Cyclohexanediol, 2-cyclohexen-1-ol and 2-cyclohexen-1-one. [c] Ti-MOR was post-prepared by treating the dealuminated sample (Si/Al = 468) with $TiCl_4$ vapor at 773 K for 1 h. 0.2 g of the catalyst was used; all the other conditions were identical. n.d. = not detected.

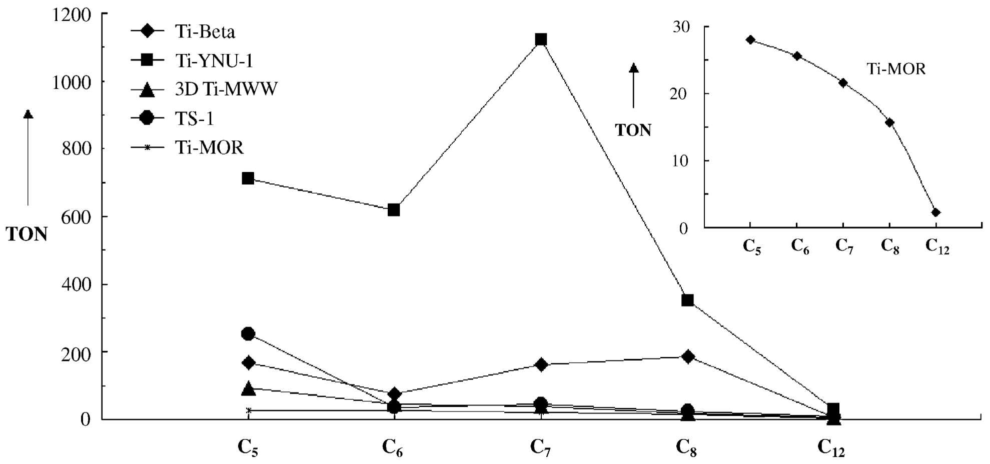

Figure 4. The turnover number (TON/(mol (mol Ti)$^{-1}$)) for the oxidation of cycloalkenes with 5–12 carbon atoms over various titanosilicate molecular sieves. For reaction conditions, see Table 1. The inset shows the TON of Ti-MOR.

much stronger intrinsic ability than TS-1 for the oxidation of linear alkenes,[6] it gave a lower TON for the oxidation of cyclopentene. This indicates that an increased steric restriction is exerted on 3D Ti-MWW, and is consequently indicative of a smaller opening in 3D Ti-MWW than in TS-1. In contrast, the catalytic activity of Ti-YNU-1 and Ti-Beta increased up to C_7 or C_8 cycloalkenes (except for cyclopentene), respectively, and then declined sharply. The activity is expected to increase with an increase in the number of carbon atoms in the cycloalkenes because of the increased number of electron-donating methyl groups on the coplanar conformation. The reason for a lower conversion of cyclohexene than that of cyclopentene on Ti-YNU-1 and Ti-Beta is probably that the reaction temperature in the oxidation of cyclopentene (333 K) is much higher than its boiling point (319 K). It can be reasonably deduced that the pore window of Ti-YNU-1 is slightly smaller than that of Ti-Beta from the fact that Ti-Beta exhibits the highest TON for cyclooctene among the cycloalkenes investigated while Ti-YNU-1 shows the highest TON for cycloheptene. For Ti-MOR, the conversion gradually declines as cycloalkenes increase in molecular size. It is reasonable to assume that the pore size of Ti-MOR is smaller than that of Ti-YNU-1 but larger than that of TS-1 since Ti-MOR shows comparable conversion for cyclopentene (10.2 %) and cyclohexene (9.0 %) but lower conversion for cycloheptene (7.5 %). This result shows that the steric constraints become important for Ti-MOR with cycloheptene. Thus, it is concluded that the effective pore size of various titanosilicate molecular sieves decreases in the order Ti-Beta > Ti-YNU-1 > Ti-MOR > TS-1 > 3D Ti-MWW. This result is consistent with the XRD characterization that showed that the layer space of Ti-YNU-1 is enlarged by about 2.5 Å as compared with 3D Ti-MWW, since the effective pore openings of Beta and mordenite zeolites are 7.1 × 7.3 Å and 7.0 × 6.5 Å, respectively, whereas that of 3D MWW is 4.0 × 5.5 Å between the layers.[16]

In summary, a new titanosilicate Ti-YNU-1, with a lamellar structure analogous to a MWW precursor, has been synthesized. It exhibits the pore properties of 12-MR zeolite and proves to be a highly active, selective, and stable catalyst in the liquid-phase epoxidation of bulky alkenes with H_2O_2.

XRD patterns of samples prepared with a synthesis gel of differing Si/Ti ratios as well as OH-region IR spectra of Ti-YNU-1 and 3D Ti-MWW are presented as Supporting Information.

Experimental Section

The lamellar precursor of the MWW titanosilicate was synthesized from highly siliceous MWW zeolite, $[Ti(OBu)_4]$, piperidine (PI), and deionized water following procedures reported elsewhere.[17] Typically, PI (7.24 g) and $[Ti(OBu)_4]$ (0.29 g) were dissolved in 22.5 g of deionized water, then highly deboronated B-MWW (5 g) was added to the above solution. The resultant mixture was heated at 443 K for 5 days under rotation. The as-synthesized precursors were then refluxed in 2 M HNO_3 solution and further calcined at 823 K for 10 h to obtain a novel lamellar titanosilicate with a structure analogous to the MWW precursor, and denoted as Ti-YNU-1.

The liquid-phase oxidation of alkenes with H_2O_2 (31 % in aqueous solution) was carried out at 333 K for 2 h while stirring in a round-bottomed flask equipped with a condenser. The temperature was controlled with a water bath. In a typical batch, catalyst (0.05 g), acetonitrile (10 mL; solvent), alkene (10 mmol; substrate), and H_2O_2 (10 mmol; oxidant) were employed. With respect to the investigation of catalytic stability, the reaction conditions were maintained for the repeat experiments, that is, reaction temperature = 333 K, reaction time = 2 h, cyclohexene/H_2O_2 = 1:1 molar ratio, 1 mL MeCN per mmol cyclohexene, 1 g catalyst per 100 mmol cyclohexene. After each run, the catalyst was centrifuge-washed with acetone and then distilled water for four times, respectively. The solid material was dried at 100 °C, and further calcined at 550 °C for 8 h before the next reaction run.

X-ray diffraction (XRD) patterns were recorded by a MAC Science M3X 1030 X-ray diffractometer with $Cu_{K\alpha}$ radiation (40 kV, 20 mA). The diffuse reflectance UV/Vis spectra (DRS) were measured on a Jasco V-550 UV/Vis spectrophotometer. OH-region infrared (IR) spectra were acquired on a PE-1600 FTIR spectrometer. Before recording the spectra in the OH region, the samples were first evacuated at 500 °C and 10^{-4} Torr for 2 h. ^{29}Si MAS NMR measurements were performed on a JEOL JNMECA 400 nuclear magnetic resonance spectrometer at ambient temperature. The chemical shift was referenced to an external standard of polydimethylsilane. The spin rate of the rotor was 5.0 kHz with a repetition time of 30 s. A pulse length of 7 μs was applied and approximately 3000 scans were accumulated. The spectra were deconvoluted with a Gaussian–Lorentzian mixed equation. The TEM images were obtained with a JEOL JEM-2000EX at 200 KV. N_2 adsorption (77 K) and H_2O adsorption (298 K) were carried out on Belsorp 28SCA and Belsorp 18SCA instruments, respectively. Thermogravimetric analysis was measured by an ULVAC-Riko TGD 9600 thermal analysis system. The chemical composition of the samples was determined with an inductively coupled plasma-atomic emission spectrometer (Shimadzu ICPS-8000E). The product was analyzed by a Shimadazu GC-14B gas chromatograph equipped with a 50 m OV-1 capillary column and a flame ionization detector. The amount of the unconverted H_2O_2 was determined by titrating with 0.1 M $Ce(SO_4)_2$ aqueous solution.

Received: August 27, 2003 [Z52723]

Keywords: alkenes · epoxidation · heterogeneous catalysis · titanosilicates · zeolites

---

[1] G. Bellussi, M. S. Rigutto, *Stud. Surf. Sci. Catal.* **1994**, *145*, 151.
[2] M. A. Camblor, A. Corma, A. Martínez, J. Pérez-Pariente, *Chem. Commun.* **1992**, 589.
[3] A. Tuel, *Zeolites* **1995**, *15*, 236.
[4] P. Wu, T. Komatsu, T. Yashima, *J. Phys. Chem.* **1996**, *100*, 10316.
[5] M. J. Díaz-Cabañas, L. A. Villaescusa, M. A. Camblor, *Chem. Commun.* **2000**, 761; A. Corma, M. J. Díaz-Cabañas, M. E. Domine, F. Rey, *Chem. Commun.* **2000**, 1725.
[6] P. Wu, T. Tatsumi, T. Komatsu, T. Yashima, *J. Catal.* **2000**, *202*, 245.
[7] A. Corma, U. Diaz, V. Fornes, J. L. Jorda, M. Domine, F. Rey, *Chem. Commun.* **1999**, 779.
[8] R. Millini, G. Perego, W. O. Parker, Jr., G. Bellussi, L. Carluccio, *Microporous Mater.* **1995**, *4*, 221.
[9] A. Corma, V. Fornes, S. B. Pergher, T. L. M. Maesen, J. G. Buglass, *Nature* **1998**, *396*, 353.
[10] G. P. Heitmann, G. Dahlhoff, W. F. Hölderich, *J. Catal.* **1999**, *186*, 12.
[11] P. Wu, T. Tatsumi, T. Komatsu, T. Yashima, *J. Phys. Chem. B* **2001**, *105*, 2897.
[12] T. Maschmeyer, F. Rey, G. Sanker, J. M. Thomas, *Nature* **1995**, *378*, 159.
[13] M. E. Leonowicz, J. A. Lawton, S. L. Lawton, M. K. Rubin, *Science* **1994**, *264*, 1910.
[14] P. Wu, W. Fan, T. Tatsumi, unpublished results.
[15] M. E. Davis, C. Chen, S. L. Burkett, R. F. Lobo, *Mater. Res. Soc. Symp. Proc.* **1994**, *346*, 831.
[16] C. Baerlocher, W. M. Meier, D. H. Olson, *Atlas of Zeolite Framework types*, Elsevier, Amsterdam, **2001**, pp. 77, 191, 203.
[17] P. Wu, T. Tatsumi, *Chem. Commun.* **2002**, 106.